CT ANGIOGRAPHY EVALUATION OF THE RENAL VASCULAR PATHOLOGIES: A PICTORIAL REVIEW

M. Oz, T. Hazirolan, B. Turkbey, A.D. Karaosmanoglu, M. Canyigit, B. Peynircioglu

The emergence of CT angiography (CTA) has a groundbreaking impact on the evaluation of renal vessels and is gradually replacing the conventional catheter angiography as the standard imaging procedure. In this review, we aimed to describe the renal CTA technique and imaging findings of several renal arterial (i.e. atherosclerosis, fibromuscular dysplasia, aneurysms of the renal arteries, dissection, vasculitidis, follow-up of patients with renal arterial stent) and venous (i.e. nut-cracker syndrome, pelvic congestion syndrome) pathologies.

Key-words: Renal veins, CT – Renal arteries, CT.

CT angiography, which is a rapid and non-invasive method, has become a widely used imaging modality in imaging of renal vascular pathologies (1, 2). The most common renal vascular pathologies include renal artery stenosis, renal artery aneurisms, dissection, vasculitiditis and fibromuscular dysplasia. At renal CT angiography, not only vascular pathologies, but also related secondary parenchymal alterations of kidneys such as infarction and atrophy can be demonstrated. Indications of renal CT angiography include imaging work-up of the diagnosis of occlusive diseases of the renal artery and related hypertension, follow up of balloon angioplasty or renal stenting, preoperative assessment of the patients that will undergo partial or total nephrectomy, post-operative follow-up, preoperative assessment of renal transplant candidate donors and acute onset flank pain in some occasions (3, 4).

Image acquisition

The diagnostic accuracy of renal CTA relies on the quality of the raw data acquired. MDCT protocol for the assessment of renal vessels consists of both unenhanced and enhanced CT scans (at arterial and venous phases). Unenhanced scan of kidneys with contiguous sections of 3-mm thickness is necessary for evaluation of vascular calcifications, and renal calculi. The optimal coverage for arterial phase scan should cover the area between the celiac artery and the terminal part of the main iliac artery (Fig. 1), but in patients with ectopic or transplanted kidney the
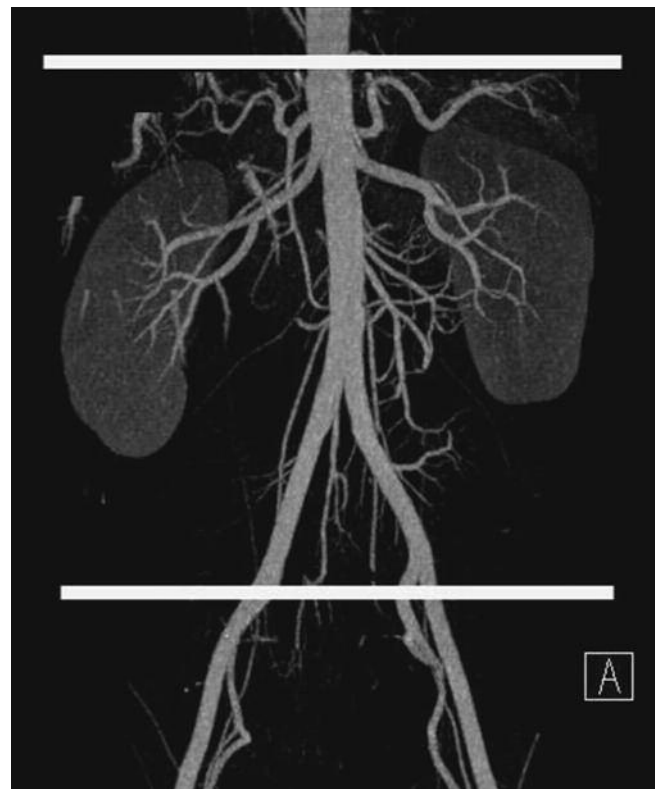

Fig. 1. — The coverage of the arterial phase, which should include abdominal aorta and main iliac arteries, where main and accessory renal arteries have their origins.

coverage can be increased. 1-1,5 mm thickness slices are obtained after intravenous injection of a 100-mL bolus of 300-400 mg/ml non-ionic iodinated contrast at a rate of 4cc/sec and 70-mL bolus at a rate of 5-6 cc/sec at 16 and 64-Channel MDCT scanners, respectively. Image acquisition is started after a delay of 4-5 and 6-7 seconds at 16 and 64-channel MDCT scanners, respectively after a

threshold enhancement of 100 HU is reached within the abdominal aorta under bolus tracking. For evaluation renal venous structures and abdominal viscera whole abdomen is scanned with a slice thickness of 5 mm following a delay of 60-80 sec after IV contrast injection. The scanning parameters are summarized in table I.

Renal artery pathologies

Renal artery stenosis

Occlusive diseases of the renal artery can result in hypertension, renal dysfunction and renal failure, ultimately. Renal artery stenosis

From: Department of Radiology, Hacettepe University School of Medicine, Ankara, Turkey.
Address for correspondence: Dr B. Turkbey, Department of Radiology, Hacettepe University School of Medicine, 06500, Sihhiye, Ankara, Turkey.
E-mail: bturkbey@yahoo.com

Table I. — MDCT scanning parameters used in renal CT angiography.

	16 MDCT			64 MDCT		
	Unenhanced	Arterial	Venous	Unenhanced	Arterial	Venous
KV/effective mass	120/140	140/140	120/140	120/160	120/150	120/160
Rotation time (sec)	0.5	0.5	0.5	0.5	0.33	0.5
Detector collimation (mm)	1.5	0.75	1.5	1.2	0.6	1.2
Slice thickness (mm)	3	1	5	3	1	5
Pitch	1.25	1.5	1.25	1.4	1.4	1.4
Reconstruction interval	3	1	5	3	0.5	5
Scan delay (sec)	0	4-5	60	0	7-8	60
Dose-length product (DLP) (mGy × cm)	6-7			5-6		

in up to 30% of patients (7) (Fig. 2).

The pathophysiology of the hypertension is the reduction in the renal perfusion associated with constriction of the renal artery resulting in the activation of the renin-angiotensin-aldosteron pathway and the sympathetic nervous system, which ultimately leads to renovascular hypertension, renal dysfunction, even to renal failure (8).

FMD is the second common cause of RAS, which is most commonly seen in females of 2nd to 5th decades (9). The distinction of FMD lesions from atherosclerotic disease is typically made by their location which is usually at mid to distal portion of the main renal artery. The disease is generally bilateral (10). In FMD, intima, media and adventitial layers of the vessel walls are all affected and in approximately 90% of cases; however, the media layer is mainly affected. The so-called "rosary beads", representing
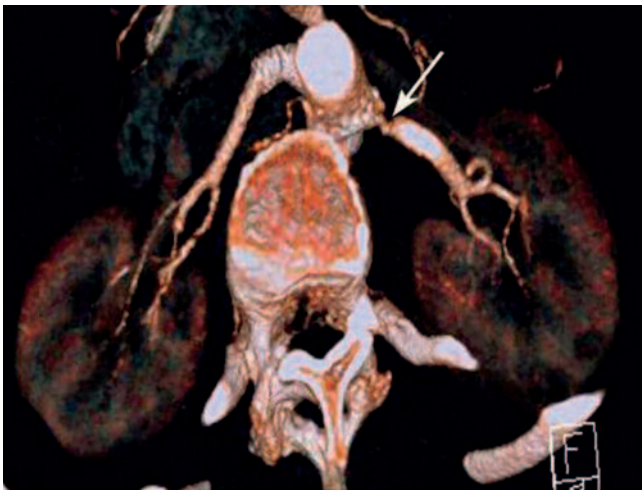

Fig. 2. — 56-year-old female with hypertension. The left renal artery stenosis is seen on volume rendered CT image (arrow).

(RAS) is responsible for secondary hypertension in 5% of adults and atherosclerosis is the most common etiology among elder population (> 55 years old), whereas fibromuscular dysplasia (FMD) is the most common cause among young individuals (5, 6). In atherosclerotic RAS, the stenosis typically occurs due to calcification and atherosclerotic plaque(s) localized to the proximal portion of the renal artery just close to the orifice, which can be bilateral

Fig. 3. — 36-year-old female with hypertension. Coronal CT angiography (A) and conventional angiography (B) images demonstrates the typical "rosary beads" pattern.

Fig. 4. — 37-year-old female with hypertension secondary to renal artery stenosis. Post stenotic dilatation (arrowhead) is seen at the distal flow tract of the stenotic segment in the middle left renal artery (arrow) at the coronal MIP images.
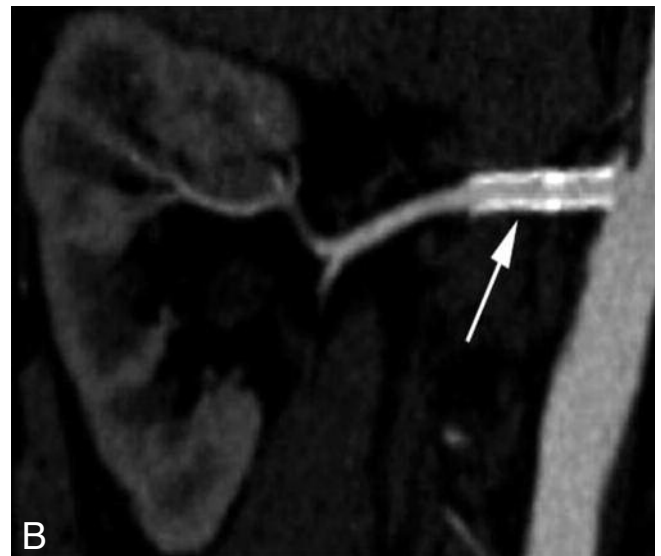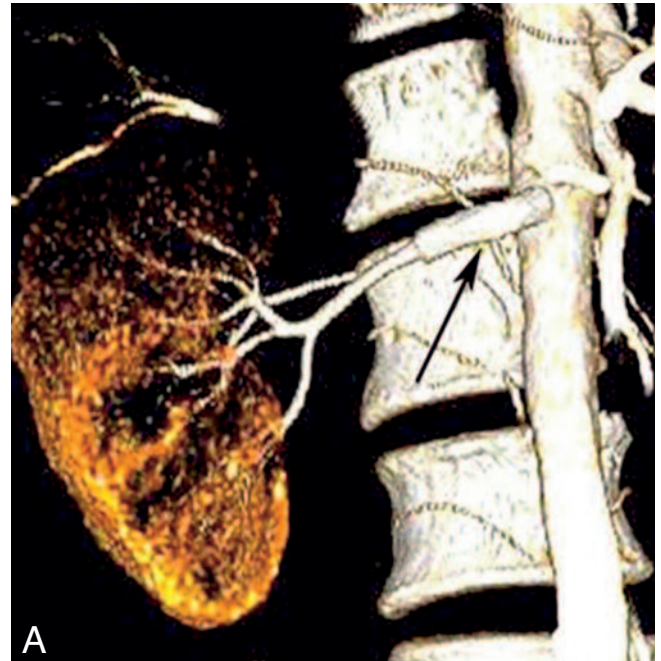

Fig. 6. — Imaging follow-up after placement of an endovascular stent for right renal artery stenosis in a 51-year-old female with atherosclerotic stenosis. Curved-MPR image demonstrates the patency of the stent (arrow).

Fig. 5. — 56-year-old male with hypertension secondary to left renal artery stenosis. Coronal CT angiography image demonstrates the difference in perfusion and the dimensions between kidneys due to chronic left renal artery stenosis.

the alternating dilated and stenosed segments, is the typical imaging finding (10, 11). Even though there are publications stressing the excellent diagnostic accuracy of CT angiography (12); careful evaluation should be made in every patient and further imaging studies (e.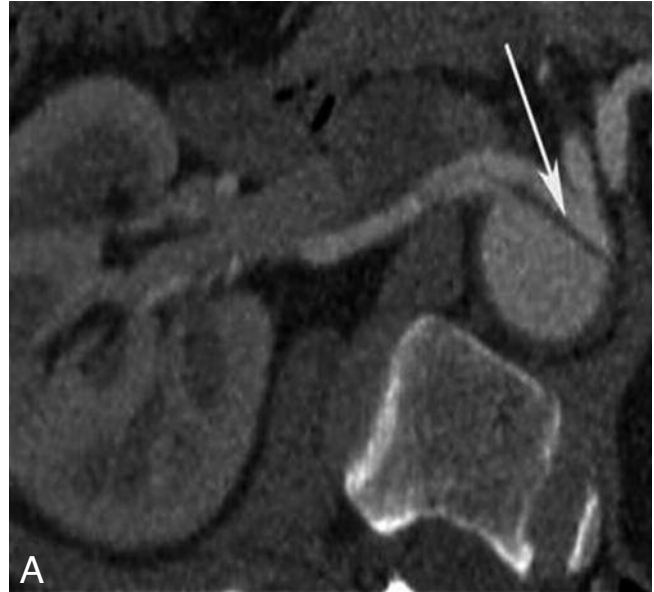g. catheter angiography) can be needed to confirm the diagnosis, specifically in young individuals and middle aged women (13) (Fig. 3).

CT angiography is a non-invasive and reliable imaging modality in the detection of RAS with sensitivity values close up to 100% in diagnosis of the severe stenosis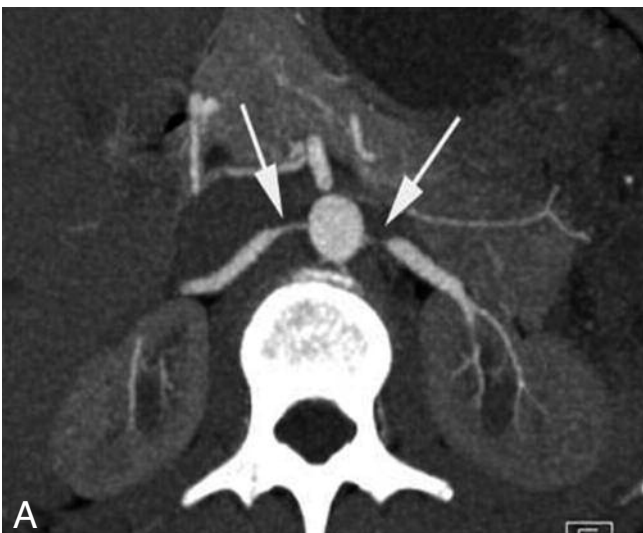 (> 50%) (14-16). Maximum intensity projection (MIP) and volume rendering techniques are both useful and complementary in the assessment of the stenosis at CT angiography. Indeed, axial images are not solely sufficient due to the tortuous nature of arteries, their variable anatomical course and presence of accessory renal arteries (14, 16). Moreover, secondary signs of the arterial stenosis such as post-stenotic dilatation (Fig. 4), differences in the parenchymal perfusion and morphological alterations (atrophy, contour changes etc.) can also be accurately assessed on CT (Fig. 5). MIP images provide angiography-like

Fig. 7. — 67-year-old male with atherosclerosis. Curved MPR CT angiography image demonstrates a calcified saccular aneurysm at the left renal hilum (arrow).
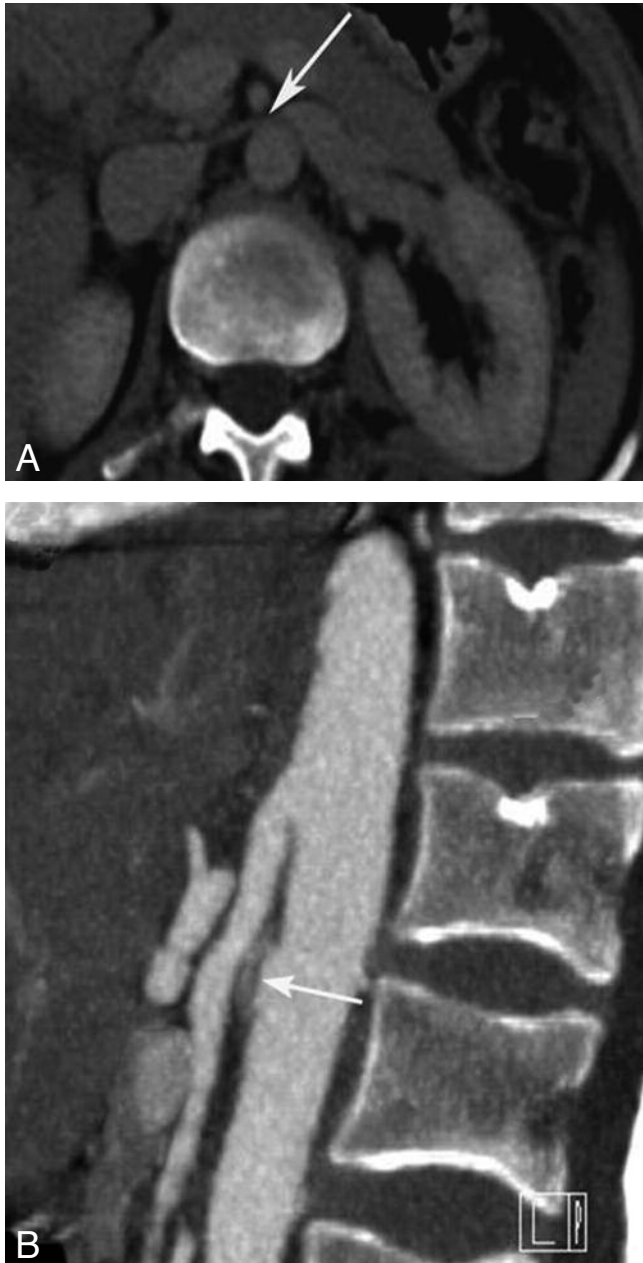

Fig. 8. — 48-year-old man with type B aortic dissection. Axial CT angiography images demonstrate an aortic dissection flap extending to right (A) and left (B) renal arteries (arrows).

images with an excellent overview of vascular anatomy and their variable projection angles should be used for accurate interpretation of stenotic lesions. Multiplanar and curved multiplanar reconstruction images are particularly useful for correct evaluation of the arterial luminal diameter for accurate depiction and quantification of the arterial stenosis, specifically in FMD.

Fig. 9. — 19-year old female with Takayasu arteritis. Axial MIP image demonstrates Takayasu arteritis affecting bilateral renal arteries (arrows) (A). Late venous phase image shows significant thickening of the aortic wall as an indicator of the active disease process (arrows) (B).

Fig. 10. — 48 year-old woman with a history of microscopic hematuria. The compression of the left renal vein at the aortico-mesenteric forks in axial unenhanced (A) and reformatted oblique sagittal CT angiography images (arrows) (B).

Fig. 11. — 39-year-old woman with an ongoing pelvic pain of two years. coronal MIP (A) and axial (B) Ct angiography images show the dilatation of the left ovarian vein (A) and pelvic varices (B) (arrows).
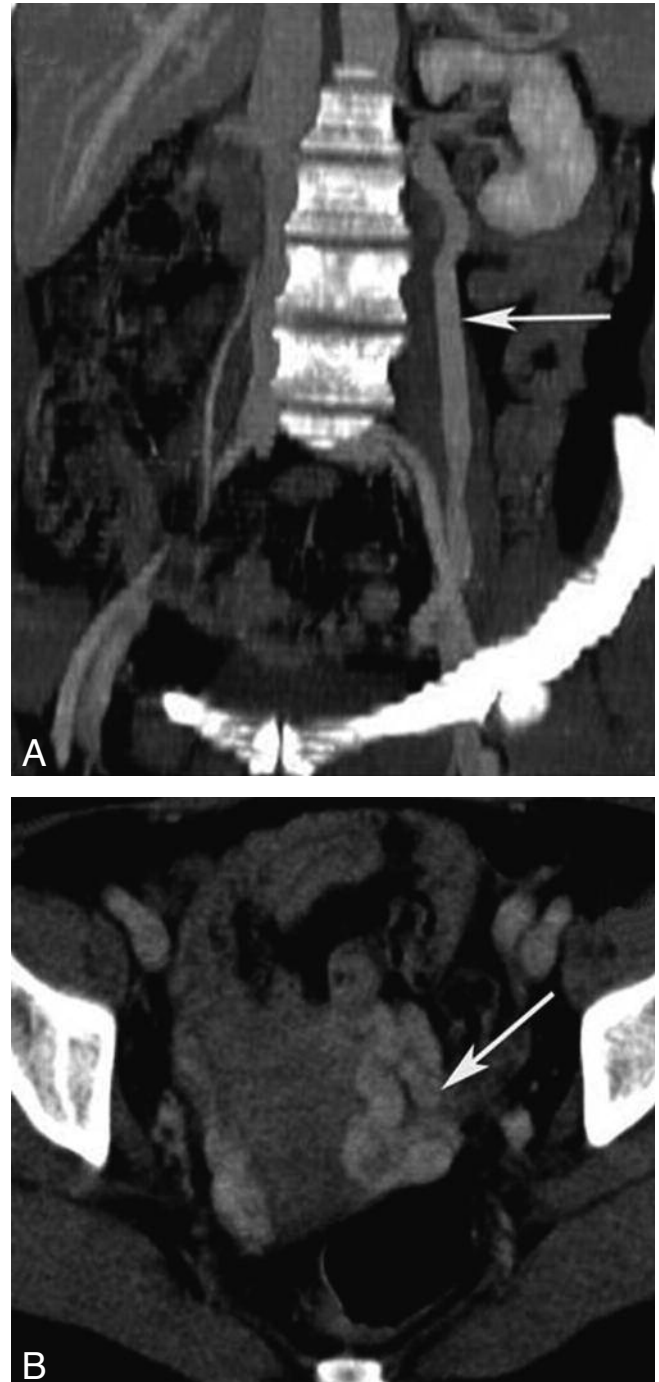
The endovascular treatment with balloon angioplasty and/or stents is almost always the first therapeutic intervention for RAS. The outcome of endovascular treatment (stent lumen patency) can be accurately assessed at CT angiography by using raw and reconstructed images (Fig. 6).

Acute occlusion of renal artery

Acute renal infarction (ARI) is a cause of acute flank pain. The most common cause is thromboem-bolism. The most common clinical manifestation is acute flank or back pain. Hematuria, proteinuria, fever, leukocytosis and an elevated serum lactate dehydrogenase may also accompany. Parenchymal changes in the kidney depend on the size of the embolus, the location of the arterial occlusion, and its age. MDCT easily demonstrates absence of enhance-ment in the affected renal tissue, which typically appears as wedge-shaped low attenuation areas (17). An additional CT finding of ARI is the cortical rim sign which represents preserved perfusion in the outer renal cortex which is supplied by renal capsular arteries (18).

Renal artery aneurysms

Renal artery aneurysms (RAA) are detected approximately in the 0.1% of the patients undergoing imaging studies, mostly in the 4th and 5th decades of the life (11, 19). The most common causes of RAA are atherosclerosis, polyarteritis nodosa, FMD and trauma (11). Morphologically, they can be saccular or fusiform in shape; a rim calcification can be also seen in 18% of them (19, 20) (Fig. 7). Less than 10% of the atherosclerotic aneurysms are symptomatic and again less than 5% of them undergo rupture, however the risk of rupture is higher in ones with a diameter of greater than 2 cm. Non-calcified RAAs and RAAs in pregnant patients are believed to be more prone to rupture (21, 22).

Renal arterial dissections

Renal artery dissection (RAD) is generally stenotic and/or occlusive in nature. Individuals with hypertension with an underlying atherosclerosis or FMD are generally more prone to have RAD. Aortic dissections may also cause constriction or occlusion by extending towards renal arteries. Acute dissections can occur as a complication of diagnostic and therapeutic catheter angiography; whereas chronic dissections may either be spontaneous or secondary to renovascular hypertension (23) (Fig. 8).

Vasculitis

Renal CT angiography is used as the first line renal vascular imaging modality in the diagnosis and follow-up of vasculitic conditions such as Takayasu disease, polyarteritis nodosa (PAN). In Takayasu disease, the thickening of the vessel wall and the luminal stenosis can be accurately assessed at CT angiography and detection of the contrast enhancement within the vessel wall can be postulated as the indicator of an active disease (Fig. 9). In PAN, microaneurysms at the interlobar or arcuate artery bifurcations, and infarct areas at different ages can be seen (24).

Renal venous pathologies

Nutcracker syndrome and pelvic congestion syndrome

Nutcracker syndrome occurs secondary to occlusion of the left renal vein between the aorticomesenteric fork (Fig. 10). The disease usually presents with asymptomatic hematuria due to increased peri-glomerular or peri-ureteral capillary pressure. In males, the reflux to the testicular vein might cause the varicosity of the pampiniform venous plexus, that may lead to secondary infertility; whereas, in females the retrograde venous flow into the ovarian veins may result in the varicose dilatation in the ovarian and parametrial venous plexuses (25).

Pelvic congestion syndrome is characterized by the dilatation pelvic venous structures secondary to retrograde blood flow from the left renal vein. It may be the cause of pelvic pain which is more prominent in erect or semi-erect postures (26) (Fig. 11).

Conclusion

MDCT angiography is currently the main imaging method in assessment of the renal vasculature. It provides highly valuable and concluding data in patients with vascular pathologies involving the renal vessels non-invasively.

References

1. Kuszyk B.S., Heath D.G., Ney D.R., et al.: CT angiography with volume rendering: imaging findings. *AJR*, 1995, 165: 445-448.
2. Smith P.A., Fishman E.K.: Three-dimensional CT angiography: renal applications. *Semin Ultrasound CT MR*, 1998, 19: 413-424.
3. Urban B.A., Ratner L.E., Fishman E.K.: Three-dimensional Volume-rendered CT Angiography of the Renal Arteries and Veins: Normal Anatomy, Variants, and Clinical Applications. *Radiographics*, 2001, 21: 373-386.
4. Fleischmann D.: Multiple detector-row CT angiography of the renal and mesenteric vessels. *Eur J Radiol*, 2003, 45: 79-87.
5. Thomsen H.S., Sos T.A., Nielsen S.: Renovascular hypertension: diagnosis and intervention. *Acta Radiol*, 1990, 30: 113-120.
6. Pickering T.G.: Renovascular hypertension: etiology and pathophysiology. *Semin Nucl Med*, 1989, 19: 79-88.
7. Bookstein J.J., Maxwell M.H., Abrams H.L., et al.: Cooperative study of radiologic aspects of renovascular hypertension. *JAMA*, 1977, 237: 1706-1709.
8. Uder M., Humke U.: Endovascular therapy of renal artery stenosis: where do we stand today? *Cardiovasc Intervent Radiol*, 2005, 28: 139-47.
9. Youngberg J.P., Sheps S.G., Strong C.G.: Fibromuscular disease of the renal arteries. *Med Clin North Am*, 1977, 61: 623-641.
10. Harrison E.G. Jr, Hunt J.C., Bernatz P.E.: Morphology of fibro-muscular dysplasia of the renal artery in renovasclar hypertension. *Am J Med*, 1967, 43: 97-112.
11. Kadir S.: Angiography of the kidneys. In: Kadir S., eds. Diagnostic angiography. Philadelphia, Pa: Saunders, 1986, 445-495.
12. Beregi J.P., Louvegny S., Gautier C., et al.: Fibromuscular dysplasia of the renal arteries: compari-son of helical CT angiography and arteriography. *AJR*, 1999, 172: 27-34.
13. Das C.J., Neyaz Z., Thapa P., Sharma S., Vashist S.: Fibromuscular dysplasia of the renal arteries: a radiological review. *Int Urol Nephrol*, 2007, 39: 233-238.
14. Johnson P.T., Halpern E.J., Kuszyk B.S., et al.: Renal artery stenosis: CT angiography-comparison of real-time volume rendering and maximum intensity projection algorithms. *Radiology*, 1999, 211: 337-343.
15. Qanadli S.D., Mesurolle B., Coggia M., et al.: Abdominal aortic aneurysm: pretherapy assessment with dual-slice helical CT angiography. *AJR*, 2000, 174: 181-187.
16. Coulier B.: Multidetector-row CT of renal arteries: review of the performances in normo- and hypertensive patients. *JBR-BTR*, 2005, 88: 311-321.
17. Akpinar E., Turkbey B., Eldem G., Karcaaltincaba M., Akhan O.: When do we need contrast-enhanced CT in patients with vague urinary system findings on unenhanced CT? *Emerg Radiol*, 2009, 16: 97-103.
18. Wong W.S., Moss A.A., Federle M.P., Cochran S.T., London S.S.: Renal infarction: CT diagnosis and correlation between CT findings and etiologies. *Radiology*, 1984, 150: 201-5.
19. Tham G., Ekelund L., Herrlin K., et al.: Renal artery aneurysms: natural history and prognosis. *Ann Surg*, 1983, 197: 348-352.
20. Tan W.A., Chough S., Saito J., Wholey M.H., Eles G.: Covered stent for renal artery aneurysm. *Catheter Cardiovasc Interv*, 2001, 52: 106-109.
21. Rundback J.H., Rizvi A., Rozenbilt G.N., et al.: Percutaneous stent-graft management of renal artery aneurysms. *J Vasc Interv Radiol*, 2000, 11: 1189-1193.
22. Yang J.C., Hye R.J.: Ruptured renal artery aneurysm during pregnancy. *Ann Vasc Surg*, 1996, 10: 370-372.
23. Williams D.M., Lee D.Y., Hamilton B.H., et al.: The dissected aorta.III.Anatomy and radiologic diagnosis of branch vessel compromise. *Radiology*, 1997, 203: 37-41.
24. Kawashima A., Sandler C.M., Ernst R.D., Tamm E.P., Goldman S.M., Fishman E.K.: CT evaluation of renovascular disease. *Radiographics*, 2000, 20: 1321-1340.
25. Beard R.W., Highman J.H., Pearce S., Reginald P.W.: Diagnosis of pelvic varicosities in women with chronic pelvic pain. *Lancet*, 1984, 2: 946-949.
26. Beard R.W., Reginald P.W., Wadsworth J.: Clinical features of women with chronic lower abdominal pain and pelvic congestion. *Br J Obstet Gynaecol*, 1988, 95: 153-161.